

## Shunt current in InAs diffused photodiodes

A.V. Sukach<sup>1</sup>, V.V. Tetyorkin<sup>1</sup>, A.I. Tkachuk<sup>2</sup>

<sup>1</sup>V. Lashkaryov Institute of Semiconductor Physics, NAS of Ukraine, Kyiv, Ukraine

<sup>2</sup>V. Vynnychenko Central Ukrainian State Pedagogical University, Kropyvnytskyi, Ukraine

E-mail: teterkin@isp.kiev.ua

**Abstract.** The shunt current has been investigated in  $p^+-n$  type InAs diffused photodiodes. The mesastructures were prepared by etching in  $\text{Br}_2\text{-HBr}$  solution and sequentially etched in CP-4 and in a lactic acid based etchants. The surface of mesastructures was passivated in alcohol solution of  $\text{Na}_2\text{S}$ . After each chemical treatment, the current-voltage and capacitance-voltage characteristics were measured as functions of bias voltage and temperature. It has been shown that the shunt current contains ohmic and non-ohmic components. The evidences have been obtained that the non-ohmic shunt current originates from the space-charge limited current in the surface inversion layer and the trap-assisted tunneling current in the bulk.

**Keywords:** InAs, shunt current, inversion surface layer.

<https://doi.org/10.15407/spqeo23.02.208>

PACS 73.40.Gk, 73.40.Kp

Manuscript received 10.02.20; revised version received 10.04.20; accepted for publication 10.06.20; published online 12.06.20.

### 1. Introduction

The key issue affecting the performance of IR photodiodes (PDs) based on narrow-gap semiconductors, including HgCdTe, InAs, InSb, is an excess dark current at low biases, commonly referred to as the shunt leakage current. The latter can reduce the threshold parameters of IR photodiodes. Moreover, since the shunt current varies unpredictably from one photodiode to another, even when they are manufactured nominally under the same conditions, the yield of photodiodes with predictable parameters suffer from this current. Traditionally, the term “shunt” is used only for ohmic resistance, and in the equivalent circuit of a photodiode it is represented by a parallel resistance [1]. In practice, the shunt resistance  $R_{sh}$  is measured at zero or small forward (reverse) bias voltages  $U \sim kT/e$  [2]. When PD is operating in photovoltaic mode, the output current is given by [3]

$$I = I_{ph} - I_d - I_{sh} = I_{ph} - I_0 \left[ \exp\left(\frac{eU - IR_s}{\beta kT}\right) - 1 \right] - \frac{eU - IR_s}{R_{sh}}, \quad (1)$$

where  $I_{ph}$  is the photocurrent,  $I_d$  – dark current and  $I_{sh}$  – shunt current,  $\beta$  – ideality coefficient. The series resistance  $R_s$  consists of the resistance of quasi-neutral regions of the junction and contacts. Because the second and third terms in this Eq. (1) reduce the linearity of photodiode, the shunt resistance should be as large as possible, whereas the series resistance should be small. In an ideal photodiode,  $R_{sh} = \infty$  and  $R_s = 0$ , so  $I = I_{ph} - I_d$ .

However, it has been shown in early studies of photovoltaic devices that shunts may have linear (ohmic) as well as non-linear (diode) current-voltage characteristics [4]. In details, the shunt current was investigated in HgCdTe photodiodes [5-7]. The relevance of this problem has been also pointed out for InAs photodiodes [8], but to authors’ knowledge the nature of the shunt current as well as the impact of surface conductivity on electrical properties of mesastructured InAs  $p-n$  junctions has not been investigated yet. Since in InAs photodiodes of  $p^+-n$  type the space charge region is located in the  $n$ -side of the junction, it was traditionally assumed that the surface conductivity of the  $p^+$ -region was not critical as compared with photodiodes possessing the symmetrically doped junction.

It should be pointed out that, in analysis of experimental results obtained in this study, the definition of shunt as a local region in the  $p-n$  junction where the dark current significantly exceeds its value in the homogeneous part is used [9, 10]. Such a definition covers both ohmic and non-ohmic shunts of different nature. Thus, the aim of this work was to study the impact of surface chemical treatment on the nature of the shunt current in the mesastructured InAs  $p^+-n$  junctions.

### 2. Samples and experimental methods

Wafers of  $n$ -InAs with the thickness approximately 1 mm were cut from an ingot grown in “Pure Metals Plant” (Svitlovodsk, Ukraine). After mechanical grinding and polishing, the damaged layers were removed using

chemical polishing with 2% Br<sub>2</sub> solution in HBr. Their structural quality was controlled using the X-ray diffraction method. In the chemically polished substrates, the rocking curve half-width was 25...27". Electrical parameters were controlled using the van der Pauw technique at 295 K. The carrier concentration and mobility were found to be  $n = (2...3) \times 10^{16} \text{ cm}^{-3}$  and  $\mu_n = (2...2.5) \times 10^4 \text{ cm}^2/\text{V}\cdot\text{s}$ , respectively. The density of dislocations was within the range  $(2...4) \times 10^4 \text{ cm}^{-2}$ . Homojunction PDs were prepared using short-term (20...30 min) diffusion of Cd into *n*-InAs substrates at 875 K. To prevent arsenic evaporation from the surface, the diffusion was carried out from the saturated cadmium vapor in the presence of arsenic. The substrates with the diffused *p*-type layer had mirror-like surfaces free of structural damages such as inclusions of impurity atoms. They were characterized by the rocking curve half-width of 32...35". Mesastructured junctions were prepared on (111)A side of substrates by chemical etching in 2% Br<sub>2</sub>-HBr solution. The mesa was formed by complete removing the diffused *p*<sup>+</sup>-type layer and part of the *n*-type conductivity substrate. The junction depth was determined from the probe thermo-emf measurements during careful chemical etching of the diffused layer. The metallurgical junction was formed close to the middle of the mesa height. The typical height of mesas was  $5 \pm 0.2 \mu\text{m}$ . After mesas etching, the samples were rinsed in deionized water for 5 min and then dried with pure hydrogen. The area of mesas was close to  $7.5 \cdot 10^{-2} \text{ cm}^2$ , and the thickness of the base region was  $\sim 660 \mu\text{m}$ . Ohmic contacts were prepared by thermal vacuum evaporation of zinc and indium on *p*-InAs, and indium on *n*-InAs substrates, followed by heat treatment in the atmosphere of pure hydrogen. After formation of mesas, the latter were etched in CP-4 solution (mixture of HF, nitric acid, acetic acid and water) and in the mixture of lactic acid, HNO<sub>3</sub> and HF [11]. Finally, these mesastructures were passivated in alcohol solution of sodium sulfide [8]. The prepared mesastructured junctions (hereafter initial, etched and passivated junctions, respectively) were tested by measuring the current-voltage and high-frequency ( $f = 1 \text{ MHz}$ ) capacitance-voltage characteristics within the temperature range 77...298 K.

### 3. Experimental results and discussion

The results of  $C-U$  measurements are shown in Fig. 1. The experimental data are satisfactorily linearized in  $C^{-3}-U$  scale for all the mesastructures, which can be explained by formation of a linearly-graded *p-n* junction. Note that the slope of the  $C^{-3}-U$  dependence for the initial mesastructure (curve 1) is significantly smaller than for the passivated one (curve 2). The cut-off voltage  $U_C \approx 1.4 \text{ V}$ , determined as an intercept on the voltage axis of the linear  $C^{-3}-U$  dependence, significantly exceeds the band gap of InAs. Such a behavior of the measured capacitance is similar to that one of MOS structure. The  $C^{-3}-U$  dependences in the etched and passivated mesastructures were similar and satisfactorily

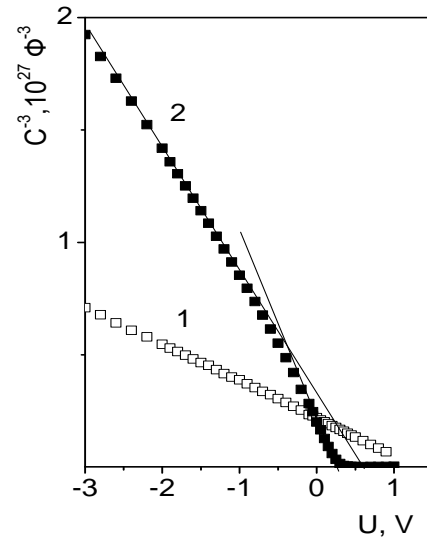


**Fig. 1.** Capacitance-voltage characteristics in the initial (1) and passivated (2) mesastructured *p*<sup>+</sup>-*n* junctions at 77 K. The straight lines are shown as a guide for the eye.

approximated by two straight lines with different slopes. This fact indicates complex distribution of impurity atoms in the junction. The cut-off voltages are different for these linear regions, namely, 0.5 and 0.35 V (see curve 2). The value  $U_C = 0.35 \text{ V}$  agrees well with the diffusion potential  $U_D$  determined from the  $I-U$  characteristics at  $T = 77 \text{ K}$  (see below). From the slope of the straight lines, the concentration gradient of impurity atoms was estimated to be  $a = 1.4 \cdot 10^{20}$  and  $1.9 \cdot 10^{20} \text{ cm}^{-4}$ , where the smaller value corresponds to the straight line with the larger slope. For the initial mesastructure,  $a$  equals  $6.8 \cdot 10^{20} \text{ cm}^{-4}$ . Note that  $C^{-3}-U$  dependence levels off in the passivated mesastructure at forward biases, which indicates the presence of compensated high resistance area at the metallurgical *p-n* junction.

The forward  $I-U$  characteristics in the initial mesastructure are shown in Fig. 2a. As seen, at bias voltages  $U \leq 80 \text{ mV}$  the forward current does not depend on temperature within the range of temperatures 77...163 K. The replotting of the experimental data in the double logarithmic scale showed the ohmic behavior of  $I-U$  curves. The shunt resistance  $R_{sh}$  approximately equals 180 Ohm for the bias voltage 50 mV at 77 K. With the bias voltage increase, the transition to an exponential  $I-U$  dependence is observed, which followed by a linear dependence due to impact of series resistance  $R_s$ . The series resistance varies from 0.8 Ohm at 77 K to 1.5 Ohm at 298 K. The forward  $I-U$  characteristics can be approximated using the following equation:

$$I = G_0 U - I_0 \exp\left(\frac{eU - IR_s}{\beta kT}\right), \quad (2)$$

where  $G_0$  is the ohmic conductivity of the shunt layer,  $I_0$  – pre-exponential factor, and  $\beta$  – ideality coefficient. Note that the value of  $\beta$  varies from 4.8 at 77 K down to 2.3 at 201 K, and 2.0 at higher temperatures.

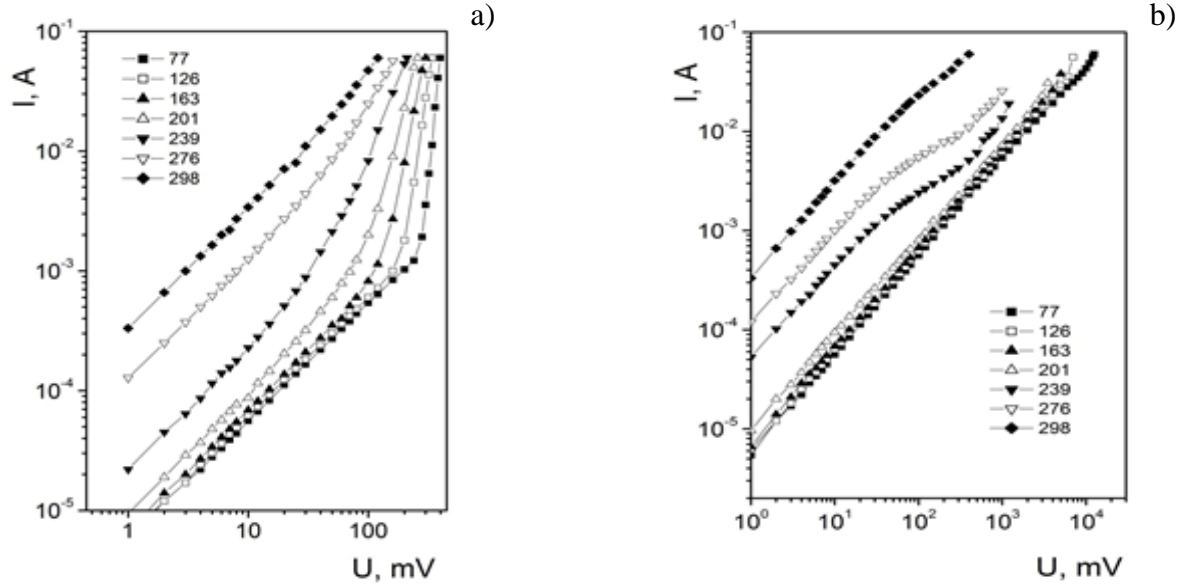


Fig. 2. Forward (a) and reverse (b) current-voltage characteristics in the initial mesastructure at different temperatures.

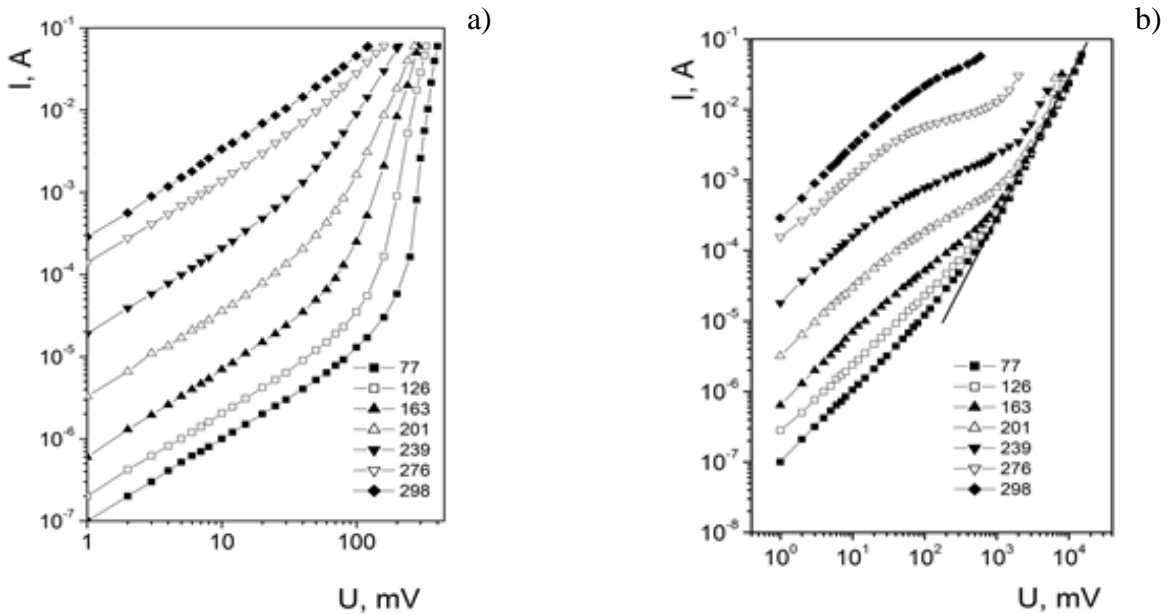
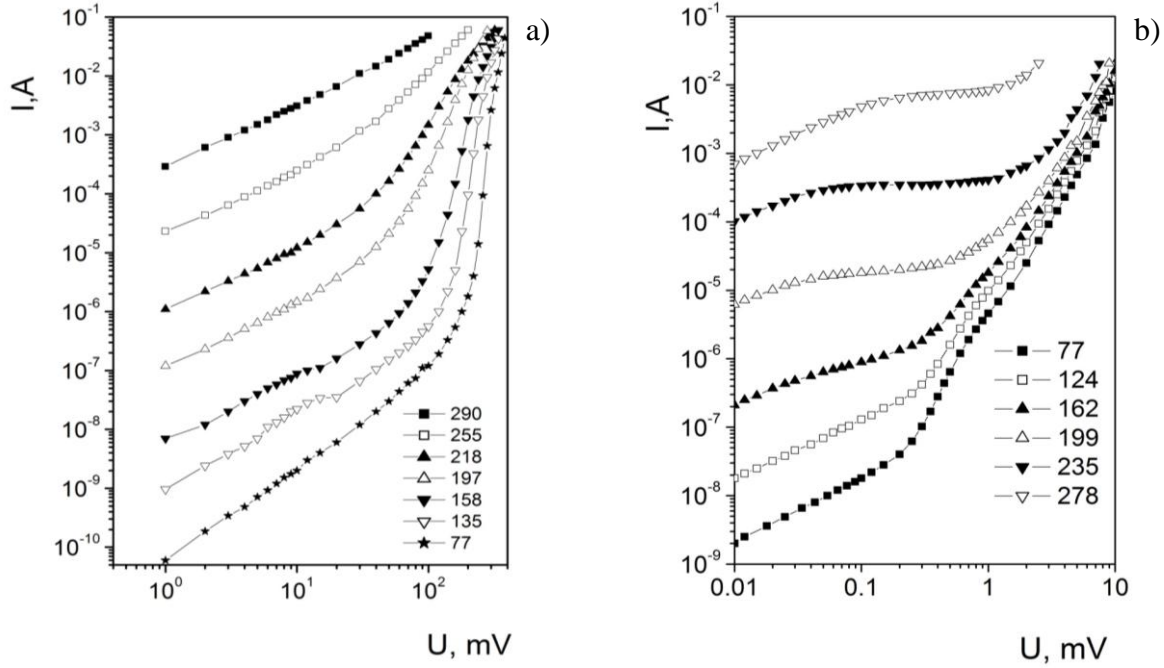


Fig. 3. Forward (a) and reverse (b) current-voltage characteristics in the mesastructure etched in lactic acid base solution at different temperatures. The straight line is shown as a guide for the eye and represents the quadratic dependence  $I \sim U^2$ .

Due to decrease in the diffusion potential with increasing temperature, the exponential part of  $I-U$  curves becomes shorter and the influence of  $R_s$  on the non-exponential behavior of  $I-U$  curves at  $T > 239$  K is observed. Taking into account the influence of  $R_s$  on the  $I-U$  characteristics, parameters  $\beta$  and  $I_0$  were evaluated.

In Fig. 2b, the reverse  $I-U$  characteristics are presented. As seen, within the temperature range 77...200 K they exhibit linear behavior in the whole range of measuring voltages and coincide in their magnitudes. At higher temperatures, the diode-like behavior is observed. Namely, linear, sublinear and superlinear

characteristics occur at bias voltages  $1 < U < 50$  mV,  $50 < U < 200$  mV and  $U > 200$  mV, respectively. The sublinear characteristics obey the power law  $I \sim U^m$  with the exponent  $m \approx 0.5$ . The shunt resistance at 77 K equals approximately 187 Ohm for the reverse and forward voltages  $U = \pm 50$  mV. This result indicates a sufficiently high concentration of charge carriers in the shunting layer and weak temperature dependence of their mobility. With the temperature increase ( $T > 200$  K), the differential resistance of the  $p-n$  junction in the whole range of reverse voltages is less than the shunt resistance and determines the output resistance of PD.



**Fig. 4.** Forward (a) and reverse (b) current-voltage characteristics in the mesastructure passivated with sodium sulfide in isopropyl alcohol.

The  $I-U$  characteristics for the etched mesastructure are shown in Figs 3a, 3b. Their specific features are as follows. The main result is that the dark current decreases approximately by two orders of magnitude. The direct  $I-U$  characteristic within the temperature range 77...163 K can be approximated by the expression

$$I = I_{01} \exp\left(\frac{eU}{E_0}\right) + I_{02} \exp\left(\frac{eU - IR_s}{\beta kT}\right), \quad (3)$$

where  $I_{01}$ ,  $I_{02}$  are the pre-exponential factors, and  $E_0$  is the characteristic energy. At 77 K, their values are  $2.9 \cdot 10^{-6}$ ,  $6.0 \cdot 10^{-13}$  A and 67 meV, respectively. The ideality coefficient  $\beta = 1.9 \dots 2.0$  for the temperature range 77...290 K, which indicates the generation-recombination mechanism of carrier transport. The reverse characteristics differ qualitatively from those in the initial mesastructures. The important fact is that at the temperatures up to approximately 200 K the current-voltage characteristics exhibit the superlinear behavior at the bias voltages  $U > 1.0$  V. Moreover, the reverse current quadratically depends on the applied bias within approximately three orders of magnitude. The charge transfer mechanism responsible for this behavior of  $I-U$  curves is the space-charge-limited current (SCLC) [12, 13]. Note that this current-voltage characteristic has not been reported in literature so far. At temperatures  $\geq 163$  K, the sublinear characteristics with the exponent  $m \geq 0.3 \dots 0.4$  are also observed, which indicates the generation mechanism of carrier transport.

The smallest values of the dark current were obtained in the passivated mesastructure, Figs 4a, 4b. The carrier transport mechanisms in InAs mesastuctured photodiodes were investigated in details previously [14, 15]. The main their results are as follows. The excess

tunneling current in the forward-biased photodiodes was satisfactorily explained in terms of inhomogeneous  $p-n$  junction that contains local areas with much higher concentration of defects. The local inhomogeneities are proved to originate from dislocations crossing the depletion region. Dislocations affect distribution of dopant impurities resulting in formation of the so-called Cottrell atmospheres. Typical values of their diameter in III-V semiconductors were of the order of  $0.5 \dots 2 \mu\text{m}$  [16]. It was assumed that the area of a local inhomogeneity should correlate with the average cross-section area of Cottrell atmospheres. Therefore, the total area of inhomogeneities is proportional to the density of dislocations. At the same time, this area is much less (several orders of magnitude) than the total junction area. Due to this reason, the parameters determined from  $C-U$  measurements refer to homogeneous parts of the junction. From the fitting calculations, the effective electric field inside the inhomogeneity regions is approximately two orders of magnitude higher than in the homogeneous part of the junction, as it was estimated. Due to the above reasons, it was concluded that the current flowing through the local inhomogeneities mainly determines the trap-assisted tunneling current in InAs photodiodes.

In order to explain the quadratic  $I-U$  characteristics in the etched mesastructures existence of an inversion surface layer should be assumed. The surface inversion layer in  $p$ -type InAs single crystals was well investigated [17]. Recently, the impact of inversion layer on the dark current in type-II InAs/GaSb superlattice photodiodes were also reported [18, 19]. The surface passivation by using ammonium sulfide solutions results in two orders of magnitude reduction of reverse dark current density in these photodiodes.

In the investigated mesastructured junctions, the Fermi level pinning above the conduction-band minimum results in formation of the inversion layer in the  $p$ -type region. As a result, electrons can be injected into this layer from the metal contact, when the junction is reverse biased. The concentration of electrons in the inversion layer critically depends on the surface treatment. In the initial mesastructure, its value is high, and the metallic-type surface conductivity is observed. As it has been shown in [20], the treatment of InAs in the lactic acid based etchant results in a small density of slow and fast surface states. In this case, the concentration of mobile carriers in the inversion layer also reduces, resulting in the lower ohmic current at low bias voltages. With increasing voltage, ohmic and injection currents become comparable and condition for the SCLC conductivity is fulfilled. The sensitivity of thin inversion layer to the SCLC conduction mechanism was discussed in the literature [21]. It was shown that in the case of thin film the level of injection and the current density can be substantially higher (by an order of magnitude) than in the bulk case. The reason for this is the reduced carrier screening due to the electric field lines spread out of the film, thus relaxing the space charge limitation of carrier injection. Because of this reason, the SCLC in InAs nanowires occurs at a much lower critical voltage as compared to bulk specimens [22, 23].

#### 4. Conclusions

It has been shown that, in InAs mesastructured  $p$ - $n$  junctions prepared by etching in  $\text{Br}_2$ -HBr solution, the surface shunt conductivity dominates the dark current. The treatment of mesastructures in the CP-4 and lactic acid base etchants significantly reduces the dark currents.

The non-ohmic shunt current in InAs mesastructured photodiodes has surface and bulk components originating from the inversion layer and the dislocation-related conductivity in the depletion region, respectively.

#### References

1. Sze S.M., Kwok K. Ng. *Physics of Semiconductor Devices*, Wiley, 2007.
2. Thompson P.R. and Larason T.C. Method of measuring shunt resistance in photodiodes. *Measurement Science Conference*, Anaheim, CA, 2001.
3. Dongaonkar S., Servaites J.D., Ford G.M. *et al.* Universality of non-Ohmic shunt leakage in thin-film solar cells. *J. Appl. Phys.* 2010. **108**. P. 124509. <https://doi.org/10.1063/1.3518509>.
4. Banerjee S. and Anderson W.A. Temperature dependence of shunt resistance in photovoltaic devices. *Appl. Phys. Lett.* 1986. **49**, No 1. P. 38–40. <https://doi.org/10.1063/1.97076>.
5. Tobin S.P., Iwasa S., Tredwell T.J.  $1/f$  noise in (Hg, Cd)Te photodiodes. *IEEE Trans. Electron. Dev.* 1980. **ED-27**, No 1. P. 43–48. <https://doi.org/10.1109/T-ED.1980.19817>.
6. Vishnu Gopal, Sudha Gupta. Temperature dependence of ohmic shunt resistance in mercury cadmium telluride junction diode. *Infrared Physics & Technology*. 2004. **45**. P. 265–271. <https://doi.org/10.1016/j.infrared.2003.11.008>.
7. Johnson S.M., Rhiger D.R., Rosbeck J.P. *et al.* Effect of dislocations on the electrical and optical properties of long wavelength infrared HgCdTe photovoltaic detectors. *J. Vac. Sci. Technol. B*. 1992. **10**. P. 1499–1503. <https://doi.org/10.1116/1.586278>.
8. Lebedev M.V., Sherstnev V.V., Kunitsyna E.V., Andreev I.A., and Yakovlev Yu.P. Passivation of infrared photodiodes with alcoholic sulfide solution. *Semiconductors*. 2011. **45**, No. 4. P. 526–529. <https://doi.org/10.1134/S1063782611040142>.
9. Breitenstein O. Understanding shunting mechanisms in silicon cells: A review. *Proc. 17<sup>th</sup> NREAL workshop on crystalline silicon solar cells and modules: materials and processes*. Colorado, August 5–8, 2007. P. 61–70.
10. Breitenstein O., Altermatt P., Ramspeck K., Green M.A., Zhao J., Schenk A. Interpretation of the commonly observed IV characteristics of c-Si cells having ideality factor larger than two. *IEEE 4th World Conference on Photovoltaic Energy Conference*. **1**. 2006. P. 879–884. <https://doi.org/10.1109/WCPEC.2006.279597>.
11. Calahorra Z., Bregman J., and Shapira Yoram. Studies of  $\text{SiO}_x$  anodic native oxide interfaces on InSb. *J. Vac. Sci. Technol. B*. 1986. **4**, No 5. P. 1195–1202. <https://doi.org/10.1116/1.583483>.
12. Lampert M.A., Mark P. *Current Injection in Solids*. Academic Press, New York, 1970.
13. Kao K.C., Hwang W. *Electrical Transport in Solids with Particular Reference to Organic Semiconductors*. Pergamon Press, Oxford. 1981.
14. Sukach A.V. and Teterkin V.V. Ultrasonic treatment induced modification of the electrical properties of InAs  $p$ - $n$  junctions. *Techn. Phys. Lett.* 2009. **35**, No. 6. P. 514–517. <https://doi.org/10.1134/S1063785009060108>.
15. Tetyorkin V., Sukach A. and Tkachuk A. InAs infrared photodiodes, In: *Advances in Photodiodes*. Edited by Gian-Franco Dalla Betta. IntechOpen. 2011. P. 427–446.
16. Biryulin P.V., Turinov V.I., Yakimov E.B. Investigation of characteristics of InSb-based photodiode linear arrays. *Semiconductors*. 2004. **38**, No 4. P. 488–503. <https://doi.org/10.1134/1.1734678>.
17. Ando T., Fowler A.B. and Stern F. Electronic properties of two-dimensional systems. *Rev. Mod. Phys.* 1982. **54**. P. 437–672. <https://doi.org/10.1103/RevModPhys.54.437>.

18. Gin A., Wei Y., Hood A., Bajowala A., Yazdanpanah V., and Razeghi M. Ammonium sulfide passivation of type-II InAs-GaSb superlattice photodiodes. *Appl. Phys. Lett.* 2004. **84**, No 12. P. 2037–2039. <https://doi.org/10.1063/1.1686894>.
19. Shin Mou, Jian V. Li, and Shun Lien Chuang. Surface channel current in InAs/GaSb type-II superlattice photodiodes. *J. Appl. Phys.* 2007. **102**. P. 066103. <https://doi.org/10.1063/1.2783767>.
20. Odendaal V., Botha J.R., and Aurent F.D. On the processing of InAs and InSb photodiode applications. *phys. status solidi (c)*. 2008. **5**, No 2. P. 580–582. <https://doi.org/10.1002/pssc.200776821>.
21. Grinberg A.A., Luryi S., Pinto M.R. and Schryer N.L. Space-charge-limited current in a film. *IEEE Trans. Electron. Dev.* 1989. **36**, No 6. P. 1162–1170. <https://doi.org/10.1109/16.24363>.
22. Talin A.A., Leonard F., Katzenmeyer A.M. *et al.* Transport characterization in nanowires using an electrical nanoprobe. *Semicond. Sci. Technol.* 2010. **25**. P. 024015. <https://doi.org/10.1088/0268-1242/25/2/024015>.
23. Katzenmeyer A.M., Leonard F., Talin A.A. *et al.* Observation of space-charge-limited transport in InAs nanowires. *IEEE Trans. Nanotechnology*. 2011. **10**, No 1. P. 92–95. <https://doi.org/10.1109/TNANO.2010.2062198>.

#### Authors and CV



physics, technology and application of narrow-gap semiconductors and infrared devices.

**Volodymyr V. Tetyorkin**, Doctor of Sciences in Physics and Mathematics, Leading Researcher at the Laboratory for Physics and Technology of Formation of Semiconductor Structures, V. Lashkaryov Institute of Semiconductor Physics, NAS of Ukraine. The area of scientific interests includes



**Andriy V. Sukach**, Senior Researcher at the Department of Semiconductor Chemistry, V. Lashkaryov Institute of Semiconductor Physics, NAS of Ukraine. The area of scientific interests includes physics and technology of infrared sensors.



**Andriy I. Tkachuk**, assistant professor at the V. Vynnychenko Central Ukrainian State Pedagogical University, Kropyvnytskyi, Ukraine. The area of scientific interests includes physics and technology of infrared devices.